

miR-26b Promotes Granulosa Cell Apoptosis by Targeting *ATM* during Follicular Atresia in Porcine Ovary

Fei Lin, Ran Li, Zeng xiang Pan, Bo Zhou, De bing Yu, Xu guang Wang, Xue shan Ma, Jing Han, Ming Shen, Hong lin Liu*

Department of Animal Genetics, Breeding and Reproduction, College of Animal Science and Technology, Nanjing Agricultural University, Nanjing, China

Abstract

More than 99% of ovarian follicles undergo atresia in mammals, but the mechanism of follicular atresia remains to be elucidated. In this study, we explored microRNA (miRNA) regulation of follicular atresia in porcine ovary. A miRNA expression profile was constructed for healthy, early atretic, and progressively atretic follicles, and the differentially expressed miRNAs were selected and analyzed. We found that miR-26b, which was upregulated during follicular atresia, increased the number of DNA breaks and promoted granulosa cell apoptosis by targeting the ataxia telangiectasia mutated gene directly *in vitro*.

Citation: Lin F, Li R, Pan Zx, Zhou B, Yu Db, et al. (2012) miR-26b Promotes Granulosa Cell Apoptosis by Targeting *ATM* during Follicular Atresia in Porcine Ovary. PLoS ONE 7(6): e38640. doi:10.1371/journal.pone.0038640

Editor: Cornelis B. Lambalk, VU University Medical Center, The Netherlands

Received: February 13, 2012; **Accepted:** May 8, 2012; **Published:** June 21, 2012

Copyright: © 2012 Lin et al. This is an open-access article distributed under the terms of the Creative Commons Attribution License, which permits unrestricted use, distribution, and reproduction in any medium, provided the original author and source are credited.

Funding: This research was supported by the Key Project of Chinese National Programs for Fundamental Research and Development (973 Program No. 2007CB947403). This work was also supported by Chinese National Natural Science Fund (No. 30901027); this activity was funded with a Research Fund for the Doctoral Program of Higher Education of China (No. 20090097120043). The funders had no role in study design, data collection and analysis, decision to publish, or preparation of the manuscript.

Competing Interests: The authors have declared that no competing interests exist.

* E-mail: liuhonglin@263.net

Introduction

Only a limited number of follicles develop to ovulation in mammals, and more than 99% of ovarian follicles undergo degeneration known as “follicular atresia” at any stage of growth and development [1,2]. Atresia is a key process that occurs in the ovary to eliminate follicles that will not ovulate. Degeneration of atretic follicles can be explained partially by apoptosis of granulosa cells, theca interna cells, and oocytes, which exhibit a condensed nuclear structure, compacted cytoplasmic organelles, decreased cell size, and DNA fragmentation [3,4]. A recent study indicated that follicular atresia is triggered by granulosa cell apoptosis [5], but the actual molecular mechanism of follicular atresia is still unknown.

MicroRNAs (miRNAs) are endogenous small noncoding RNAs of approximately 22 nucleotides in length [6] that can partially negatively regulate gene expression at posttranscriptional level by degrading or deadenylating target mRNA or by inhibiting translation. miRNA sequences are highly conserved between species. Since *lin-4* and *let-7* were found respectively in *Caenorhabditis elegans* in 1993 and 2000 [7,8], numerous miRNAs have been identified in many animals, plants, and viruses (<http://www.mirbase.org/>) [9,10]. miRNAs play important roles in a large variety of biological and cellular processes such as development, differentiation, proliferation, apoptosis, and tumorigenesis [11,12,13], but the mechanism of miRNA regulation has yet to be elucidated. Although miRNAs have been demonstrated to take part in a wide range of physiological process, no data on the relationship between miRNAs and follicular atresia have been reported until now.

Many studies have been conducted on follicular atresia in pigs, and many factors are reported to take part in this process such as

tumor necrosis factor (TNF) [14], TNF-related apoptosis-inducing ligand [15], Fas ligand [16], X-linked inhibitor of apoptosis protein (XIAP) [17]. However, whether miRNA, an important epigenetic strategy to regulate gene expression, is applicable to the regulation of pig follicle atresia is unclear. In this study, we evaluated miRNA expression in porcine ovarian follicles using a miRNA microarray assay. Dozens of differentially expressed miRNAs were identified, and the target genes and the functions of these miRNAs were predicted. Then, we focused on the differential expression of miR-26b, which was upregulated during atresia. We found that miR-26b could induce pig granulosa cell apoptosis *in vitro*, that ataxia telangiectasia mutated (*ATM*) was a direct target gene of miR-26b, and that DNA breaks increased in granulosa cells transfected with miR-26b.

Results

miRNA Expression Profiles During Follicular Atresia in Porcine Ovary

The μ Paraflo™ miRNA microarray assay was used to evaluate the expression profiles of 1251 mature miRNAs during pig follicular atresia (Figure 1). They were composed of three parts: 1053 unique mature miRNAs from pig, human, and mouse (based on Sanger miRBase release 13.0, marked by species); 99 miRNA sequences from references (marked by R) [18,19,20]; and 99 pig miRNA candidates predicted in our laboratory (marked by P) [21]. In total, 329, 369, and 435 miRNAs were detected in the healthy (H), early atretic (EA), and progressively atretic (PA) follicles, respectively. Nearly 200 differentially expressed miRNAs ($P < 0.01$) were identified by ANOVA. The EA/H value was used for further screening because we focused on the initiation of

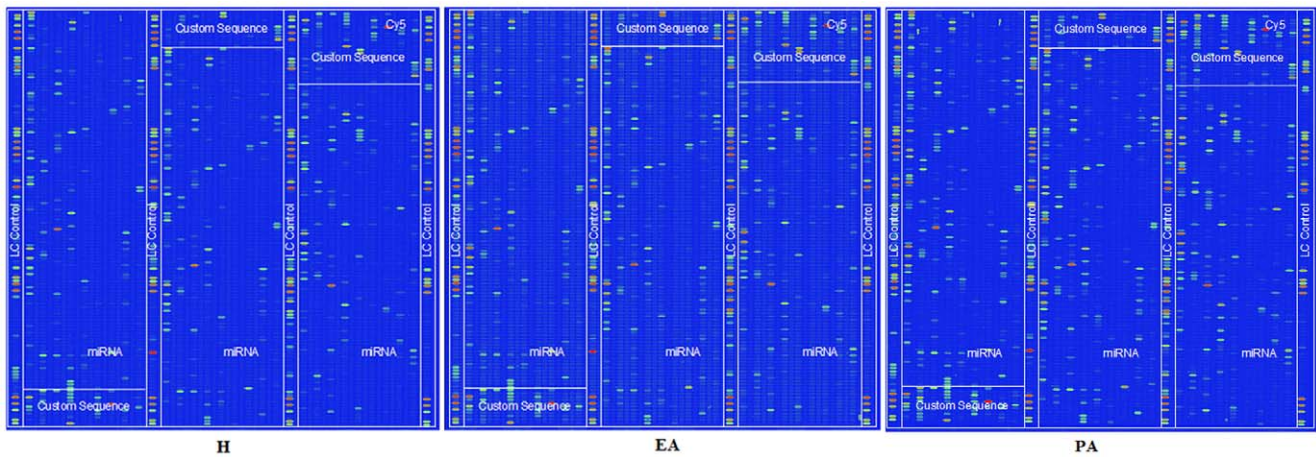


Figure 1. miRNA expression profile during porcine follicular atresia. Healthy (H), early atretic (EA), progressively atretic (PA) are representative regions of the Cy5 chip images. The images are displayed in pseudo-colors to expand the visual dynamic range. As the signal intensity increased from 1 to 65,535, the corresponding color changed from blue to green to yellow and red.
doi:10.1371/journal.pone.0038640.g001

follicular atresia. 23 miRNAs (at least one signal value >1000 with an EA/H >2 or an EA/H <0.7) were selected (Table 1), 12 of which were upregulated and 11 of which were downregulated.

Table 1. Differentially expressed miRNAs during porcine follicle atresia.

miRNA	H Mean	EA Mean	PA Mean	EA/PA	p-value
Upregulated miRNAs					
hsa-miR-936	319.67	1282.51	1003.06	4.01	1.70526E-05
P-miR-1281	464.38	1675.19	2167.30	3.61	3.70351E-06
hsa-miR-26b	172.13	561.54	1623.17	3.26	1.40894E-06
mmu-miR-1224	945.32	3012.84	2676.98	3.19	0.00056122
hsa-miR-10b	723.69	1760.22	2311.29	2.43	8.94694E-06
P-miR-466g-b	1205.42	2842.93	1363.18	2.36	0.002424305
P-miR-1275	1396.46	3030.95	1666.71	2.17	0.00172605
hsa-miR-574-5p	640.70	1375.41	293.17	2.15	0.000333658
R-miR-26b	1803.18	3869.54	9927.83	2.15	3.80023E-05
hsa-miR-149*	488.54	1025.32	1320.74	2.10	0.003760175
hsa-miR-1275	1414.95	2912.71	2052.27	2.06	0.000699006
hsa-miR-99a	353.72	708.64	1956.51	2.00	3.57687E-05
Downregulated miRNAs					
R-let-7a	41,704.41	29,099.82	15,432.83	0.70	1.18518E-05
hsa-let-7i	6930.18	4812.24	3630.25	0.69	0.000108401
hsa-miR-92b	910.77	613.02	658.31	0.67	0.002838088
hsa-miR-92a	6692.46	4483.72	2836.03	0.67	4.37391E-06
P-miR-923	37,929.77	25,246.05	13,029.16	0.67	1.67734E-07
hsa-miR-1979	32,600.93	19,093.57	8068.98	0.59	5.4785E-07
R-miR-739	43,558.83	22,871.56	11,358.65	0.53	2.24742E-06
hsa-miR-1308	7470.44	3576.30	2243.58	0.48	6.97377E-07
hsa-miR-1826	68,631.36	31,756.20	17,899.43	0.46	5.60287E-07
P-miR-1826	125,609.86	51,011.88	26,731.74	0.41	1.24318E-08
ssc-miR-184	1395.88	517.12	91.29	0.37	2.89758E-07

H, healthy; EA, early atretic; PA, progressively atretic.
doi:10.1371/journal.pone.0038640.t001

Target Genes and Functions of Differentially Expressed miRNAs

Target genes were used to predict the functions of these differentially expressed miRNAs. After the GO and Pathway analysis, 324 significant target genes (Figure S1) were selected with widespread roles in cell processes such as cell proliferation, differentiation, adhesion, apoptosis, and DNA replication (Figure S2). Let-7a and miR-26b, with target gene numbers 83 and 73 respectively, were the two most prevalent miRNAs. Seven miRNAs (let-7a, miR-26b, miR-10b, miR-1275, miR-1308, miR-1826, and miR-936) seemed to be involved in apoptosis. The miRNAs and their target genes included in apoptosis pathway are shown in Table 2. miR-26b was upregulated during follicular atresia with many predicted target genes, and may be involved in apoptosis based on the miRNA-GO and miRNA-Pathway analysis. Moreover, miR-26b suppresses cell growth and induces cell apoptosis *in vitro* [22], so it was chosen for further research.

miR-26b was Upregulated During Follicular Atresia

We first focused on the expression level of mature miR-26b in H, EA, and PA follicles. The miRNA array assay showed that

Table 2. miRNAs involved in the apoptosis pathway.

microRNAs	Target genes	Pathway name
R-let-7a	BCL2L1	Apoptosis
R-let-7a	CASP3	Apoptosis
R-let-7a	PPP3CA	Apoptosis
R-let-7a	TNFSF6	Apoptosis
hsa-miR-26b	ATM	Apoptosis
hsa-miR-26b	PPP3R1	Apoptosis
hsa-miR-1826	NFKB1	Apoptosis
hsa-miR-1826	XIAP	Apoptosis
hsa-miR-1308	BCL2	Apoptosis
hsa-miR-936	CAD	Apoptosis

doi:10.1371/journal.pone.0038640.t002

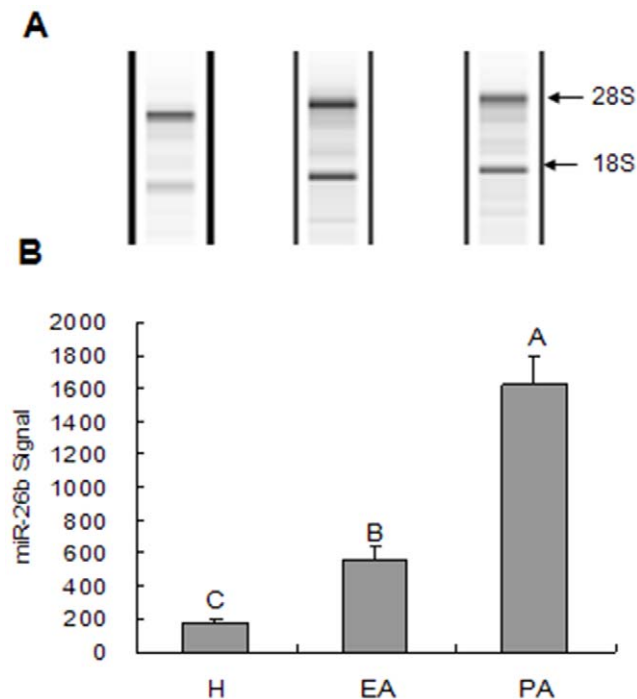


Figure 2. miR-26b expression during follicular atresia. miR-26b expression was detected by miRNA microarray assay. A, The quantity of RNA used in the microarray assay, and the integrity of 18 s and 28 s rRNA was checked. B, miR-26b signals were detected in healthy (H), early atretic (EA), and progressively atretic (PA) follicles. miR-26b expression was upregulated during porcine follicular atresia. doi:10.1371/journal.pone.0038640.g002

miR-26b was upregulated during follicular atresia in porcine ovarian follicles (Figure 2).

miR-26b Promotes Granulosa Cell Apoptosis in Vitro

Granulosa cell apoptosis is involved in follicular atresia [5,23]. We verified the effect of miR-26b on cultured granulosa cell *in vitro* to investigate the role of miR-26b during follicular atresia. Porcine granulosa cells were transfected with the miR-26b mimic or scrambled oligonucleotide. After a 72-h incubation, the cells transfected with the miR-26b mimic died by apoptosis and were floating in the medium; however, cells transfected with the scrambled oligonucleotide grew well (Figure 3A). Anti-annexin V-propidium iodide (PI) staining and FACS analysis confirmed that cell apoptosis increased significantly after transfection of the miR-26b mimic (Figure 3B and C). These data suggest that miR-26b promotes granulosa cell apoptosis.

ATM is a Target of miR-26b

ATM may be a target gene for miR-26b based on a bioinformatics analysis. To focus on *ATM* expression after miR-26b mimic treatment, we transfected porcine granulosa cells with the miR-26b mimic, scrambled oligonucleotide, or scrambled oligonucleotide marked with FAM to reflect transfection efficiency (>90%) (Figure 4A). After a 72-h incubation, we checked *ATM* expression by real-time PCR and found that the miR-26b mimic decreased *ATM* expression at the mRNA level (Figure 4B).

While exploring the mechanism for the downregulated *ATM* expression by miR-26b, a potential binding site for miR-26b was found on the *ATM* mRNA at position 5555 (NM_001123080) (Figure 5A). We hypothesized that miR-26b represses *ATM*

expression through this site, so we constructed two reporter vectors including luciferase cDNA followed by an miR-26b binding site or mutant miR-26b binding site (Figure 5B and C) as a control. The reporter vectors were co-transfected into granulosa cells with miR-26b mimic or scrambled oligonucleotide. miR-26b decreased luciferase activity of the reporter vector containing the wild-type binding site, but not the reporter with the mutant response element. In contrast, the scrambled oligonucleotide had no effect on luciferase activity of the wild-type reporter or the mutant vector (Figure 5D). Taken together, miR-26b inhibited *ATM* expression directly by binding to its mRNA at position 5555.

DNA Break Increased after miR-26b Transfection

ATM plays an important role in DNA repair [24]. If miR-26b promotes cell apoptosis by targeting *ATM*, then DNA breaks must increase after miR-26b mimic transfection. To explore the effect of miR-26b on DNA breaks, we performed the TUNEL (Terminal-deoxynucleotidyl Transferase Mediated Nick End Labeling) assay in porcine granulosa cells cultured *in vitro*. Granulosa cells with DNA breaks increased significantly in the miR-26b mimic transfection group (Figure 6). Therefore, miR-26b induced an increase in the number of DNA breaks in porcine granulosa cells *in vitro*.

Discussion

Gonadotropins [25], gonadal hormones [26,27], growth factors [28], cell adhesion molecules [29], and cell death ligands and receptors [5] are involved in follicular atresia. Our results showed that miRNA, an important epigenetic strategy to regulate gene expression, also contributed to follicular atresia. Because known porcine miRNAs are rare, we performed a miRNA microarray assay of human, mouse, and predicted porcine miRNA candidates to evaluate the expression of miRNAs during follicular atresia in pigs. miRNA expression profiles have been reported for fibroblast cells [30], muscle and adipose tissue [31], and the intestine of pigs [32], however, we conducted a miRNA microarray assay in follicles, and more than 400 miRNAs were expressed in the pig ovary. 23 differentially expressed miRNAs that may be associated with atresia were identified, the functions of these differentially expressed miRNAs remain to be studied. Although the majority was not accepted in porcine by miRBase 13.0, homologous porcine miRNAs were identified and are included in miRBase 16.0. These miRNAs were miR-1224, miR-10b, miR-574, miR-99a, let-7a, let-7i, miR-92a, and miR-92b. let-7a suppressed cancer cell death by targeting caspase-3 [33] and suppressing miR-184 could induce apoptosis [34]. These results agreed with our data, which made our result believable.

Porcine genes are highly homologous to humans, so we performed a target gene scan for miRNA in the human genome. Pro-survival and pro-apoptotic molecules are involved in ovarian apoptosis [35] and a delicate balance between them determines the final destiny of follicular cells [36]. In this study, hundreds of target genes were pretested, tens of which were involved in apoptosis, including pro-apoptosis genes (such as *CASP3* and *TNFSF6*) and anti-apoptosis genes (such as *BCL2* and *XLAP*). This suggested that miRNAs are involved in the regulation of pro-survival and pro-apoptotic gene balance. One miRNA can target numerous genes, and one gene can be regulated by several miRNAs. Our data showed that let-7a and miR-26b targeted as many as 83 and 73 genes, respectively, and that nemo-like kinase was simultaneously regulated by let-7a, miR-26b, miR-92a, and miR-936. More attention should be paid to miRNAs with more

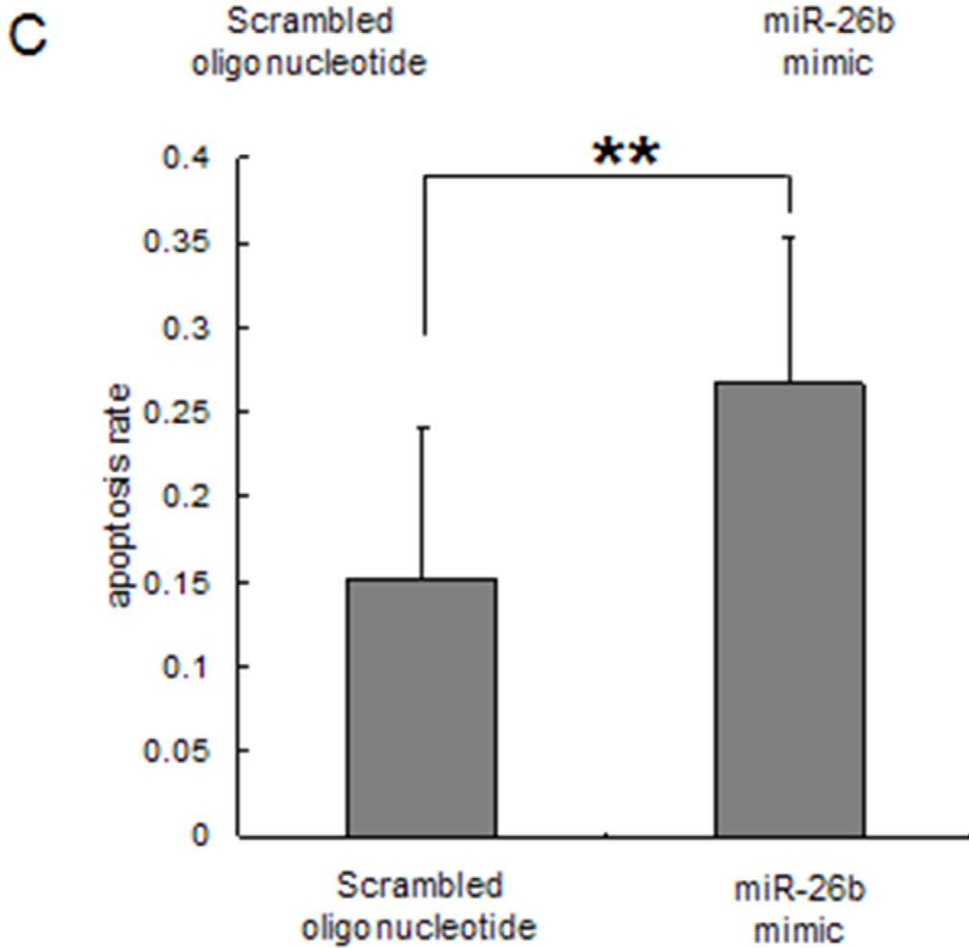
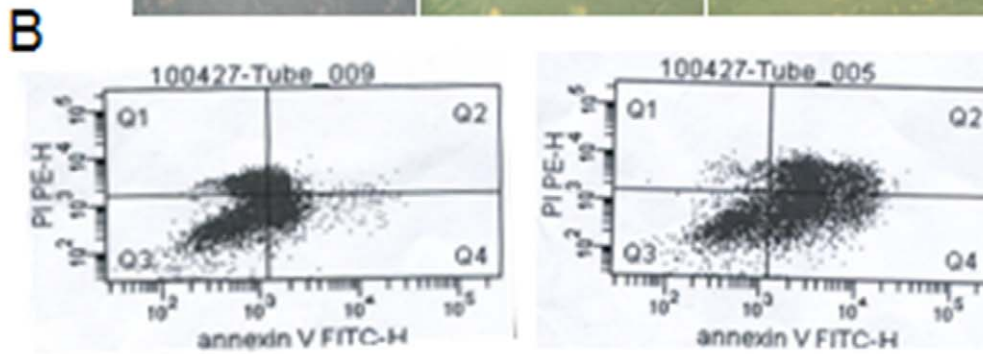
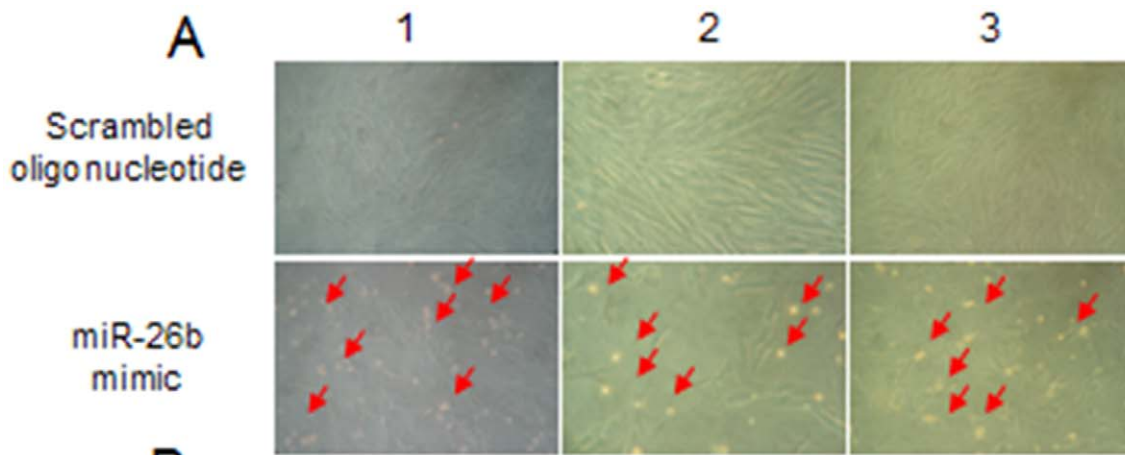


Figure 3. The effect of miR-26b on granulosa cell apoptosis *in vitro*. A, Porcine granulosa cells undergo apoptosis after miR-26b mimic treatment (three replicates). Granulosa cells were transfected with the miR-26b mimic or scrambled oligonucleotide (150 nM) after an additional 72-h culture (red arrow shows apoptosis cells). B and C, flow cytometry analysis (FACS) of apoptosis. After treatment and additional culture, cells were harvested and stained with Anti-annexin V-propidium iodide followed by FACS analysis. Apoptosis improved significantly following the miR-26b transfection.
doi:10.1371/journal.pone.0038640.g003

apoptosis-related target genes, including let-7a, miR-26b, mir-1826, and miR-936. These miRNAs are more likely to play roles during follicular atresia, but their functions remain to be determined.

Although miR-26b has not been accepted in porcine by miRBase 16.0 until now, miR-26b is expressed in pig skeletal muscles and is found in RNA pools from the heart, thymus, and liver [20,37]. Our results suggested that miR-26b was also

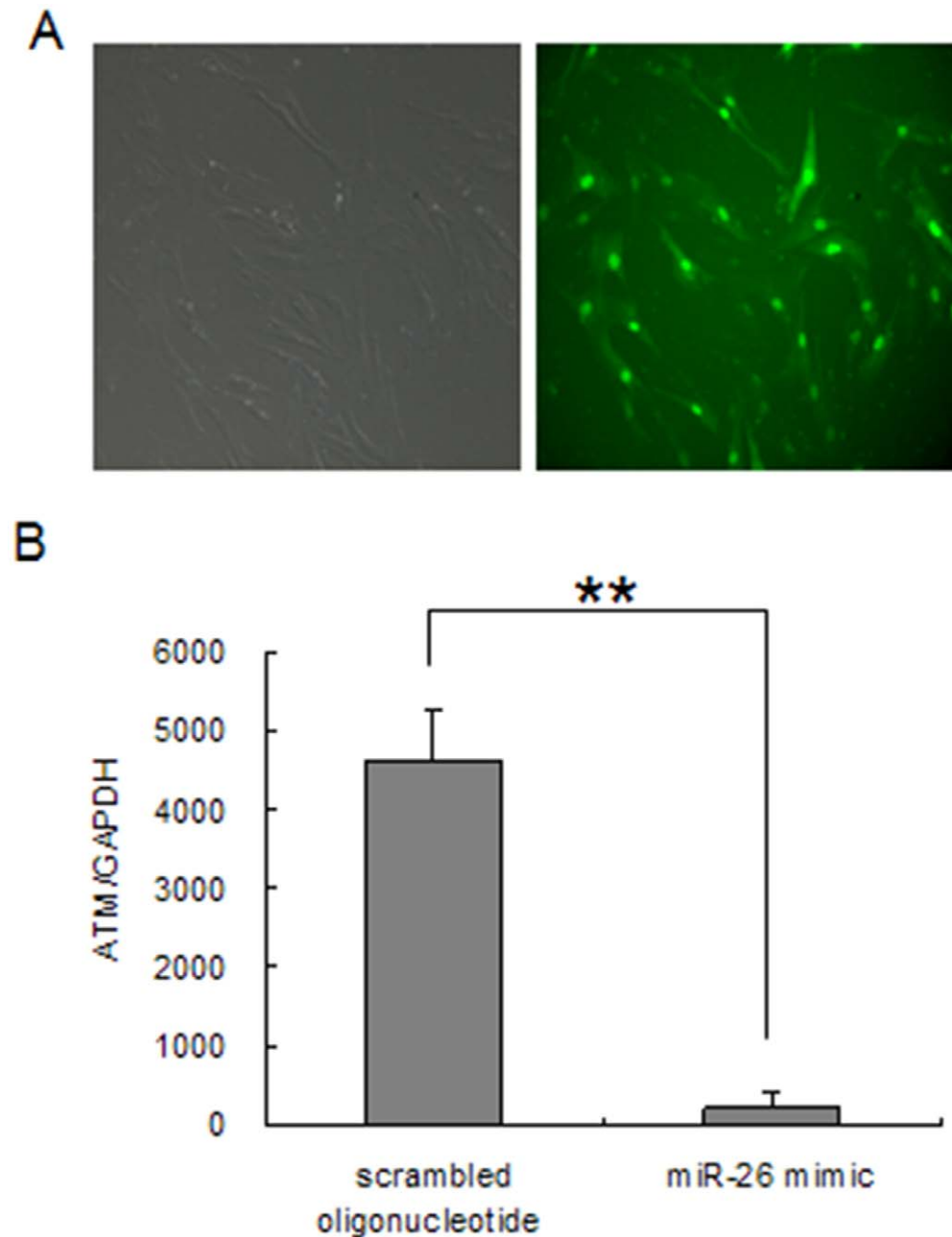


Figure 4. Regulation of ataxia telangiectasia mutated gene (*ATM*) expression by miR-26b. A, Transfection efficiency. Granulosa cells were transfected with a scrambled oligonucleotide marked with FAM (150 nM), and fluorescence was checked within 12 h after transfection. B, *ATM* expression was downregulated by miR-26b. Granulosa cells were transfected with scrambled oligonucleotide or an miR-26b mimic, and *ATM* expression was checked by real-time PCR (** $P < 0.01$ compared to the scrambled oligonucleotide).
doi:10.1371/journal.pone.0038640.g004

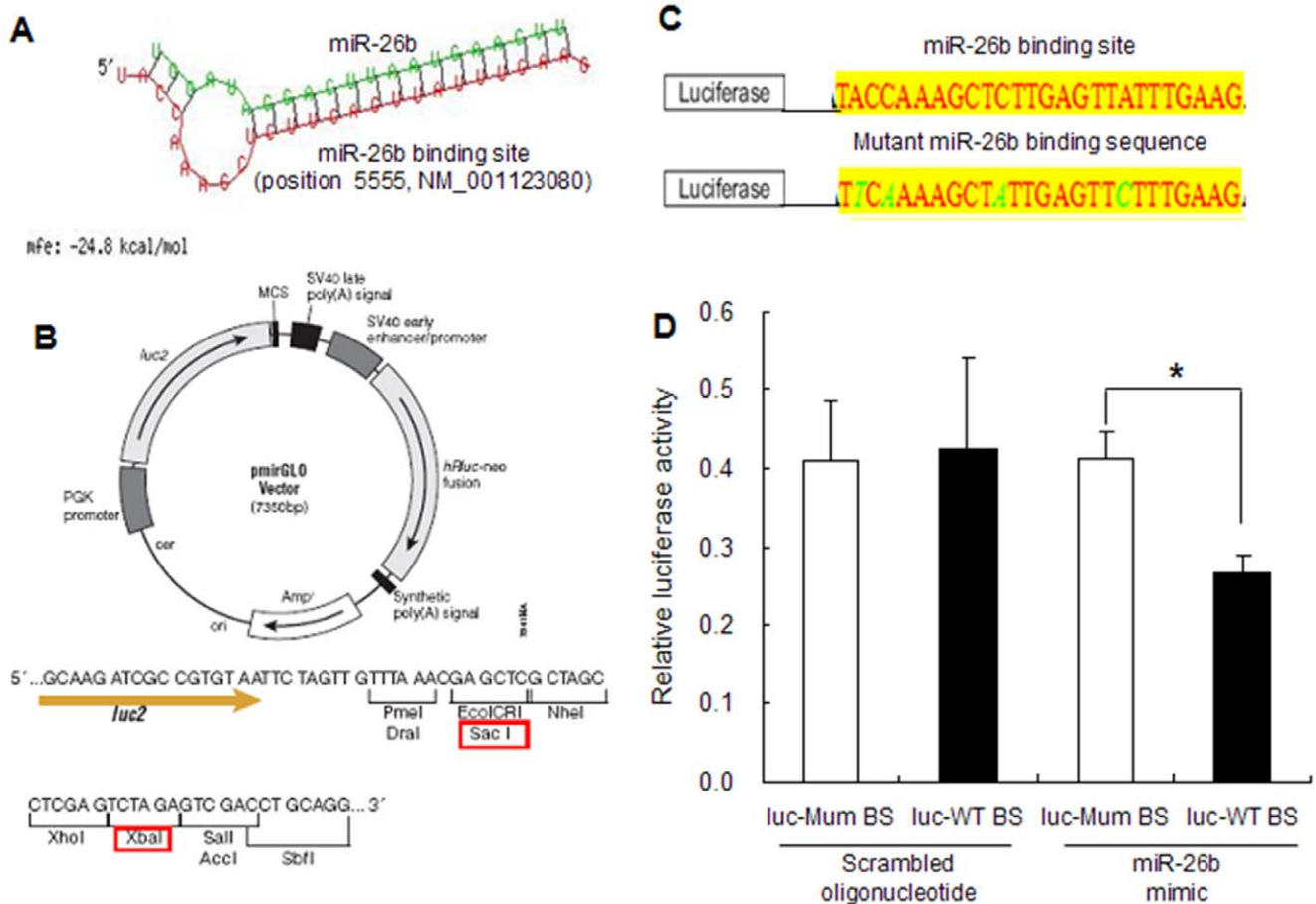


Figure 5. miR-26b binding site within *ATM* mRNA mediates downregulation of *ATM* by miR-26b. A, A miR-26b binding site within *ATM* mRNA was predicted by RNAhybrid. B, Map of the pmirGLO luciferase reporter vector. The red rectangles show the restrictive endonuclease used for cloning. C, miR-26b binding sequence for the wild type and mutant (shown in green). D, Luciferase activity assay. Granulosa cells were transfected with luciferase vectors including the wild-type or mutant miR-26b binding site and the miR-26b mimic or a scrambled oligonucleotide and harvested for the dual luciferase reporter assay after 24 h. BS, binding site. doi:10.1371/journal.pone.0038640.g005

expressed in porcine ovary and was upregulated during follicular atresia. The function of miR-26b is unclear because few studies have investigated this miRNA. miR-26b regulates pituitary development by targeting lymphoid enhancer factor 1 [38] and is downregulated in cancers [39,40]. miR-26b suppresses cell growth, induces apoptosis *in vitro* [22], and inhibits cell proliferation by regulating cyclooxygenase-2 expression [41]. Our results demonstrated that miR-26b promotes porcine granulosa cell apoptosis by targeting a member protein of the phosphatidylinositol-3-kinase-like enzyme family [42], *ATM*, which is mutated in the human disease ataxia telangiectasia.

Although the apoptosis rate improved significantly after miR-26b mimic transfection, it was not upregulated as much as we expected. This may be due to the observation that DNA breaks occur naturally without genotoxic agent treatment, as in this study. The other reasonable explain of this phenomenon is that *ATM* was downregulated by miR-26b, and that residual *ATM* may still have been expressed in granulosa cells. We demonstrated that miR-26b downregulated *ATM* directly and that reduced *ATM* expression induced granulosa cell apoptosis *in vitro*. An associated *in vivo* study was conducted using *ATM* knockout as early as 1996. *ATM*-deficient mice were infertile, and ovaries from mutant females were devoid of primordial and maturing follicles and oocytes [43], indicating that an *ATM* deficiency not only promotes apoptosis in

granulosa cells but also in oocytes, as *ATM* plays an important role in DNA repair [24]. In agreement with this result, the pathologies associated with *ATM* disease are attributable largely to defective DNA double-strand break recognition and repair [44]. Thus, DNA breaks increased greatly after the miR-26b mimic transfection.

In conclusion, a miRNA expression profile was constructed during porcine follicular atresia, and candidate miRNAs regulating follicle atresia were chosen. miR-26b increased the number of DNA breaks by targeting the *ATM* gene and promoting porcine granulosa cell apoptosis *in vitro*.

Materials and Methods

Ethics Statement

All experiments were performed according to Nanjing Agricultural University Animal Care and Use Committee guidelines and all animal work was approved by the committee. All pigs were killed in a state of unconsciousness, and then ovaries were taken.

Animal and Follicle Separation

Porcine ovaries were obtained from mature sows at a local slaughterhouse (Tianhuan Company) and transferred to the laboratory as soon as possible in physiological saline at 30°C–35°C. Individual preovulatory antral follicles (3–5 mm in diam-

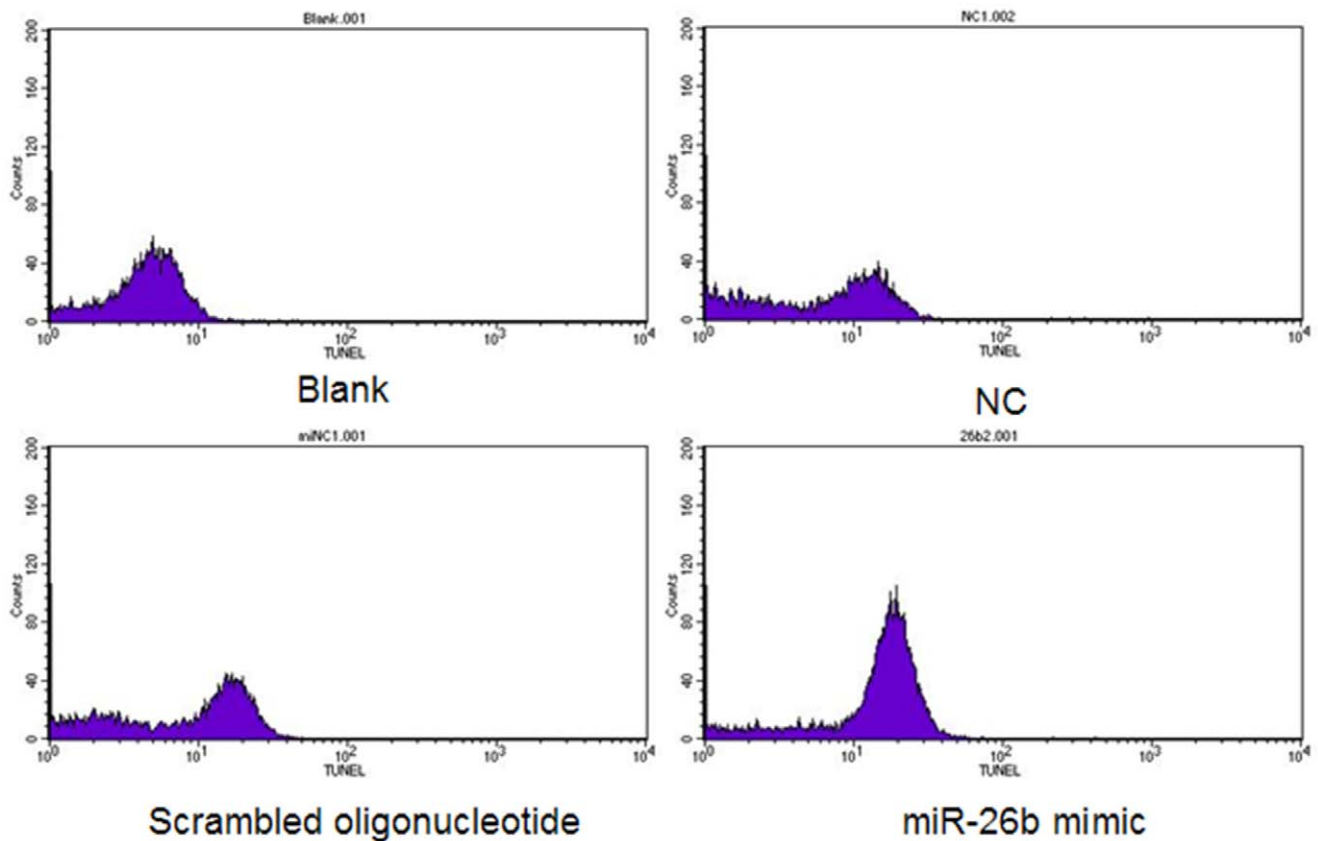


Figure 6. DNA breaks analysis by terminal deoxyribonucleotidyl transferase-mediated dUTP nick end labeling (TUNEL) assay. Granulosa cells were transfected with the miR-26b mimic or a scrambled oligonucleotide (150 nM) after an additional 72-h incubation. Cells were harvested for TUNEL stain and flow cytometry analysis. Blank, cells not transfected and without TUNEL stain; NC, cells not transfected. doi:10.1371/journal.pone.0038640.g006

eter) were dissected from the ovaries under a surgical dissecting microscope (SZ40; Olympus, Tokyo, Japan) with small scissors and forceps. Each follicle was classified morphologically as healthy (H), early atretic (EA), or progressively atretic (PA) [17,45]. Briefly, healthy follicles were round with a sharp and continuous granulosa cell membrane; they had a fixed and visible cumulus-oocyte complex [46] and clear follicular fluid. Early atretic follicles may still have a visible COC but with gaps in membrane granulosa cells and turbid follicular fluid. PA follicles did not have a visible COC or had a COC in follicular fluid with dark floccules [47,48].

Chemiluminescence for 17 β -estradiol (E₂) and Progesterone (P₄) Levels in Follicular Fluid

Follicular fluid was collected and centrifuged at 3000 \times g for 5 min to separate granulosa cells. An aliquot of each sample was diluted 100-fold with double-distilled water. The diluted fluid was used to quantify E₂ and P₄ levels using E₂ and P₄ kits (Beckman, Fullerton, CA, USA), respectively, at the General Hospital of the Nanjing Military Command. The P₄/E₂ (P/E) value was used to confirm the follicle classification [49]. The E₂ and P₄ levels in follicles selected for the miRNA microarray assay are shown in Table 3. Only follicles with P/E values in accordance with morphology were selected.

μ Paraflo™ MicroRNA Microarray Assay

The microarray assay was conducted using a service provider (LC Sciences, Houston, TX, USA). The assay used from 2 to 5 μ g

Table 3. Follicle information used in the miRNA microarray assay.

	Follicle number	P (pg/ml)	E (pg/ml)	P/E	Diameter (mm)	Morphology
H	1	1091.2	886.3	1.2	5.0	H
	2	1333.4	816.6	1.6	4.5	H
	3	1487.4	1016.5	1.5	4.0	H
	4	3824.0	1871.7	2.0	5.0	H
	5	2493.7	1187.8	2.1	4.0	H
EA	1	987.4	119.3	8.3	5.2	EA
	2	1195.0	121.5	9.8	3.2	EA
	3	1116.4	135.6	8.2	5.0	EA
	4	1292.5	179.5	7.2	3.0	EA
PA	1	1220.1	86.1	14.2	4.5	PA
	2	1440.3	114.1	12.6	4.5	PA
	3	1940.3	73.8	26.3	4.0	PA
	4	2091.2	75.2	27.8	5.3	PA
	5	1081.8	84.2	12.9	4.0	PA

doi:10.1371/journal.pone.0038640.t003

of total RNA. Hybridization was performed overnight on a μ Paraflo™ microfluidic chip using a micro-circulation pump

[50,51]. The hybridization used 100 μ l 6 \times SSPE buffer (0.90 M NaCl, 60 mM Na₂HPO₄, 6 mM EDTA, pH 6.8) containing 25% formamide at 34°C. Hybridization images were collected and digitized. Data were analyzed by first subtracting the background and then normalizing the signals using a locally weighted regression filter [52].

Potential Targets and Functions of Differentially Expressed miRNAs

Target gene, GO, and Pathway analyses were performed by the Shanghai Qiming Information Technology Company. (Shanghai, China). After targeted gene prediction, the GO analysis was applied to analyze the main function of the differentially expressed miRNAs according to Gene Ontology, which is the key functional classification of NCBI. Pathway analysis was used to identify the significant differential gene pathways, according to KEGG, Biocarta, and Reatome.

Granulosa Cell Culture and miRNA Transfection

Granulosa cells were collected from porcine ovaries using a syringe; they were washed with PBS and cultured in DMEM/F12 (1:1) with 10% fetal bovine serum in an incubator with 5% CO₂ in air at 37°C. Penicillin (100 units/ml) and streptomycin (100 μ g/ml) were used in the cultures. A miR-26b mimic and scrambled oligonucleotides were obtained from GenePharma (Shanghai, China). Granulosa cells were transfected with the miR-26b mimic or scrambled oligonucleotide (150 nM) for 6 h using Lipofectamine 2000. All experiments were repeated in triplicate.

Apoptosis Analysis

Granulosa cells were transfected with the miR-26b mimic or scrambled oligonucleotide as a control. After an additional 72-h incubation, the cells were harvested, stained with propidium iodide and anti-annexin V-FITC, and analyzed by flow cytometry to determine the relative amount of AnnexinV-FITC positive and PI-negative cells.

Real-time PCR

Total RNA was extracted using TRIZOL, and the RT reactions were performed with MLV, according to the manufacturer's protocol. Real-time PCR was amplified with SYBR Premix Ex Taq in a reaction volume of 20 μ l. Primer sequences were as follows: *ATM*, forward primer 5'-GGCTGTCACCTGATA-GAGGG-3' and reverse primer 5'-AAGGCAACTTAGGG-TAGGA-3', 243 bp; *GAPDH*, forward primer 5'-GGACTCAT-GACCACGGTCCAT-3' and reverse primer 5'-TCAGATCCAC AACCGACACGT-3', 220 bp.

Plasmid Construction

The predicted miR-26b binding site (italics), with the *SacI/XbaI* enzyme site and the sequence CTAGGATCCCTTATAC-

CAAAGCTCTTGAGTTATTTGAAGATAAT was synthesized, re-annealed, and cloned into the *SacI/XbaI* site of the pmirGLO luciferase vector. The pmir-GLO luciferase vector contained the mutant miR-26b binding site, whose sequence was CTAGGATCCCTTATTTCAAAGCTCTTGAGTTCTTTGAAGATAAT (the four italic and bold nucleotides are mutated); it was constructed simultaneously.

Luciferase Assay

Granulosa cells were plated in 6-well plates. The next day, 1000 ng/ml pmirGLO luciferase vector, including the wild-type or mutant miR-26b binding site and 50 pmol/ml miR-26b mimic or scrambled oligonucleotide, was transfected using Lipofectamine 2000. Luciferase assays were performed using the dual luciferase reporter assay system 24 h after transfection.

TUNEL Assay

The terminal deoxyribonucleotidyl transferase mediated dUTP nick end labeling (TUNEL) method, which examines DNA strand breaks, was conducted with the In Situ Cell Death Detection Kit (Roche Applied Science, Shanghai, China). Flow cytometry was also performed to detect DNA breaks in cells.

Statistical Analysis

All results are expressed as means \pm SE. The statistical analysis was performed with a *t*-test to compare two groups, and an analysis of variance (ANOVA) was applied for multiple comparisons. A *P*<0.05 was considered statistically significant.

Supporting Information

Figure S1 Potential targets prediction for differential expression miRNAs.

(TIF)

Figure S2 GO analysis of potential targets.

(TIF)

Acknowledgments

We thank Lei Chen for image processing assistance. The English in this document has been checked by at least two professional editors, both native speakers of English. For a certificate, please see: <http://www.textcheck.com/certificate/qQDA99>.

Author Contributions

Conceived and designed the experiments: HLL FL. Performed the experiments: FL RL JH MS XGW XSM. Analyzed the data: ZXP BZ DBY. Contributed reagents/materials/analysis tools: MS JH. Wrote the paper: FL.

References

- Dailey RA, Clark JR, First NL, Chapman AB, Casida LE (1975) Loss of follicles during the follicular phase of the estrous cycle of swine as affected by genetic group and level of feed intake. *J Anim Sci* 41: 835–841.
- Maeda A, Inoue N, Matsuda-Minehata F, Goto Y, Cheng Y, et al. (2007) The role of interleukin-6 in the regulation of granulosa cell apoptosis during follicular atresia in pig ovaries. *J Reprod Dev* 53: 481–490.
- Guthrie HD, Cooper BS, Welch GR, Zakaria AD, Johnson LA (1995) Atresia in follicles grown after ovulation in the pig: measurement of increased apoptosis in granulosa cells and reduced follicular fluid estradiol-17 beta. *Biol Reprod* 52: 920–927.
- Arends MJ, Morris RG, Wyllie AH (1990) Apoptosis. The role of the endonuclease. *Am J Pathol* 136: 593–608.
- Manabe N, Matsuda-Minehata F, Goto Y, Maeda A, Cheng Y, et al. (2008) Role of cell death ligand and receptor system on regulation of follicular atresia in pig ovaries. *Reprod Domest Anim* 43 Suppl 2: 268–272.
- Bartel DP (2004) MicroRNAs: genomics, biogenesis, mechanism, and function. *Cell* 116: 281–297.
- Lee RC, Feinbaum RL, Ambros V (1993) The *C. elegans* heterochronic gene *lin-4* encodes small RNAs with antisense complementarity to *lin-14*. *Cell* 75: 843–854.
- Reinhart BJ, Slack FJ, Basson M, Pasquinelli AE, Bettinger JC, et al. (2000) The 21-nucleotide *let-7* RNA regulates developmental timing in *Caenorhabditis elegans*. *Nature* 403: 901–906.
- Griffiths-Jones S, Saini HK, van Dongen S, Enright AJ (2008) miRBase: tools for microRNA genomics. *Nucleic Acids Res* 36: D154–158.

10. Ambros V, Bartel B, Bartel DP, Burge CB, Carrington JC, et al. (2003) A uniform system for microRNA annotation. *RNA* 9: 277–279.
11. Wang Y, Lee CG (2009) MicroRNA and cancer—focus on apoptosis. *J Cell Mol Med* 13: 12–23.
12. Lynam-Lennon N, Maher SG, Reynolds JV (2009) The roles of microRNA in cancer and apoptosis. *Biol Rev Camb Philos Soc* 84: 55–71.
13. Bueno MJ, de Castro IP, Malumbres M (2008) Control of cell proliferation pathways by microRNAs. *Cell Cycle* 7: 3143–3148.
14. Nakayama M, Manabe N, Inoue N, Matsui T, Miyamoto H (2003) Changes in the expression of tumor necrosis factor (TNF) alpha, TNFalpha receptor (TNFR) 2, and TNFR-associated factor 2 in granulosa cells during atresia in pig ovaries. *Biol Reprod* 68: 530–535.
15. Inoue N, Manabe N, Matsui T, Maeda A, Nakagawa S, et al. (2003) Roles of tumor necrosis factor-related apoptosis-inducing ligand signaling pathway in granulosa cell apoptosis during atresia in pig ovaries. *J Reprod Dev* 49: 313–321.
16. Inoue N, Maeda A, Matsuda-Minehata F, Fukuta K, Manabe N (2006) Expression and localization of Fas ligand and Fas during atresia in porcine ovarian follicles. *J Reprod Dev* 52: 723–730.
17. Cheng Y, Maeda A, Goto Y, Matsuda F, Miyano T, et al. (2008) Changes in expression and localization of X-linked inhibitor of apoptosis protein (XIAP) in follicular granulosa cells during atresia in porcine ovaries. *J Reprod Dev* 54: 454–459.
18. Huang TH, Zhu MJ, Li XY, Zhao SH (2008) Discovery of porcine microRNAs and profiling from skeletal muscle tissues during development. *PLoS One* 3: e3225.
19. McDaneld TG, Smith TP, Doumit ME, Miles JR, Coutinho LL, et al. (2009) MicroRNA transcriptome profiles during swine skeletal muscle development. *BMC Genomics* 10: 77.
20. Reddy AM, Zheng Y, Jagadeeswaran G, Macmil SL, Graham WB, et al. (2009) Cloning, characterization and expression analysis of porcine microRNAs. *BMC Genomics* 10: 65.
21. Zhou B, Liu HL, Shi FX, Wang JY (2010) MicroRNA expression profiles of porcine skeletal muscle. *Anim Genet* 41: 499–508.
22. Ma YL, Zhang P, Wang F, Moyer MP, Yang JJ, et al. (2010) Human embryonic stem cells and metastatic colorectal cancer cells shared the common endogenous human microRNA-26b. *J Cell Mol Med*.
23. Rolaki A, Drakakis P, Millings S, Loutradis D, Makrigiannakis A (2005) Novel trends in follicular development, atresia and corpus luteum regression: a role for apoptosis. *Reprod Biomed Online* 11: 93–103.
24. Bernstein C, Bernstein H, Payne CM, Garewal H (2002) DNA repair/pro-apoptotic dual-role proteins in five major DNA repair pathways: fail-safe protection against carcinogenesis. *Mutat Res* 511: 145–178.
25. Craig J, Orisaka M, Wang H, Orisaka S, Thompson W, et al. (2007) Gonadotropin and intra-ovarian signals regulating follicle development and atresia: the delicate balance between life and death. *Front Biosci* 12: 3628–3639.
26. Hutz RJ, Dierschke DJ, Wolf RC (1990) Role of estradiol in regulating ovarian follicular atresia in rhesus monkeys: a review. *J Med Primatol* 19: 553–571.
27. Hillier SG, Tetsuka M (1997) Role of androgens in follicle maturation and atresia. *Baillieres Clin Obstet Gynaecol* 11: 249–260.
28. Chun SY, Eisenhauer KM, Minami S, Hsueh AJ (1996) Growth factors in ovarian follicle atresia. *Semin Reprod Endocrinol* 14: 197–202.
29. Makrigiannakis A, Coukos G, Blaschuk O, Coutifaris C (2000) Follicular atresia and luteolysis. Evidence of a role for N-cadherin. *Ann N Y Acad Sci* 900: 46–55.
30. Kim J, Cho IS, Hong JS, Choi YK, Kim H, et al. (2008) Identification and characterization of new microRNAs from pig. *Mamm Genome* 19: 570–580.
31. Cho IS, Kim J, Seo HY, Lim do H, Hong JS, et al. (2010) Cloning and characterization of microRNAs from porcine skeletal muscle and adipose tissue. *Mol Biol Rep* 37: 3567–3574.
32. Sharbati S, Friedlander MR, Sharbati J, Hoeke L, Chen W, et al. (2010) Deciphering the porcine intestinal microRNA transcriptome. *BMC Genomics* 11: 275.
33. Tsang WP, Kwok TT (2008) Let-7a microRNA suppresses therapeutics-induced cancer cell death by targeting caspase-3. *Apoptosis* 13: 1215–1222.
34. Wong TS, Liu XB, Wong BY, Ng RW, Yuen AP, et al. (2008) Mature miR-184 as Potential Oncogenic microRNA of Squamous Cell Carcinoma of Tongue. *Clin Cancer Res* 14: 2588–2592.
35. Matsuda-Minehata F, Inoue N, Goto Y, Manabe N (2006) The regulation of ovarian granulosa cell death by pro- and anti-apoptotic molecules. *J Reprod Dev* 52: 695–705.
36. Hussein MR (2005) Apoptosis in the ovary: molecular mechanisms. *Hum Reprod Update* 11: 162–177.
37. Nielsen M, Hansen JH, Hedegaard J, Nielsen RO, Panitz F, et al. (2010) MicroRNA identity and abundance in porcine skeletal muscles determined by deep sequencing. *Anim Genet* 41: 159–168.
38. Zhang Z, Florez S, Gutierrez-Hartmann A, Martin JF, Amendt BA (2010) MicroRNAs regulate pituitary development, and microRNA 26b specifically targets lymphoid enhancer factor 1 (Lef-1), which modulates pituitary transcription factor 1 (Pit-1) expression. *J Biol Chem* 285: 34718–34728.
39. Porkka KP, Pfeiffer MJ, Waltering KK, Vessella RL, Tammela TL, et al. (2007) MicroRNA expression profiling in prostate cancer. *Cancer Res* 67: 6130–6135.
40. Volinia S, Calin GA, Liu CG, Ambs S, Cimmino A, et al. (2006) A microRNA expression signature of human solid tumors defines cancer gene targets. *Proc Natl Acad Sci U S A* 103: 2257–2261.
41. Ji Y, He Y, Liu L, Zhong X (2010) MiRNA-26b regulates the expression of cyclooxygenase-2 in desferrioxamine-treated CNE cells. *FEBS Lett* 584: 961–967.
42. Shafman T, Khanna KK, Kedar P, Spring K, Kozlov S, et al. (1997) Interaction between ATM protein and c-Abl in response to DNA damage. *Nature* 387: 520–523.
43. Barlow C, Hirotsune S, Paylor R, Liyanage M, Eckhaus M, et al. (1996) Atm-deficient mice: a paradigm of ataxia telangiectasia. *Cell* 86: 159–171.
44. Abraham RT, Tibbetts RS (2005) Cell biology. Guiding ATM to broken DNA. *Science* 308: 510–511.
45. Bjersing L (1967) On the ultrastructure of follicles and isolated follicular granulosa cells of porcine ovary. *Cell and Tissue Research* 82: 173–186.
46. Bortol R, Tazzari PL, Cappellini A, Tabellini G, Billi AM, et al. (2003) Constitutively active Akt1 protects HL60 leukemia cells from TRAIL-induced apoptosis through a mechanism involving NF-kappaB activation and cFLIP(L) up-regulation. *Leukemia* 17: 379–389.
47. Carson RS, Findlay JK, Burger HG, Trounson AO (1979) Gonadotropin receptors of the ovine ovarian follicle during follicular growth and atresia. *Biol Reprod* 21: 75–87.
48. Hay MR, Cran DG, Moor RM (1976) Structural changes occurring during atresia in sheep ovarian follicles. *Cell Tissue Res* 169: 515–529.
49. Manabe N, Imai Y, Ohno H, Takahagi Y, Sugimoto M, et al. (1996) Apoptosis occurs in granulosa cells but not cumulus cells in the atretic antral follicles in pig ovaries. *Experientia* 52: 647–651.
50. Gao X, Gulari E, Zhou X (2004) In situ synthesis of oligonucleotide microarrays. *Biopolymers* 73: 579–596.
51. Zhu Q, Hong A, Sheng N, Zhang X, Matejko A, et al. (2007) microParaflo biochip for nucleic acid and protein analysis. *Methods Mol Biol* 382: 287–312.
52. Bolstad BM, Irizarry RA, Astrand M, Speed TP (2003) A comparison of normalization methods for high density oligonucleotide array data based on variance and bias. *Bioinformatics* 19: 185–193.